Changes in the physical structure and chain dynamics of elastin network in homocysteine-cultured arteries

Valérie Samouillan,[1] Edouard Lamy,[2,3] Jany Dandurand,[1] Alexandrine Foucault-Bertaud,[2,3] Corinne Chareyre,[2,3] Colette Lacabanne,[1] Philippe Charpiot[2,3]

[1]*Laboratoire de Physique des Polymères, Institut Carnot, CIRIMAT UMR 5085, Université Paul Sabatier, 118 route de Narbonne, 31062 Toulouse Cedex04, France*

[2]*Inserm, UMR-S 608, Marseille, F-13005 France*

[3]*Univ de la Méditerranée, Marseille, F-13005 France*

Abstract: The thermal and dielectric properties of the elastin network were investigated in arteries cultured with physiological and pathological concentrations of homocysteine, an aminoacid responsible of histological impairments in human arteries. The physical structure of this amorphous protein was investigated by differential scanning calorimetry (DSC). To explore the molecular dynamics of the elastin network in the nanometer range, we used thermally stimulated currents (TSC), a dielectric technique running at low frequency, and measuring the dipolar reorientations in proteins subjected to a static electrical field. Combining DSC and TSC experiments reveals the molecular mobility of the proteins, both in the glassy state and in the liquid state. Significant differences are evidenced in the physical structure and relaxation behavior of elastin network in cultured arteries (physiological and pathological concentrations of homocysteine) and discussed.

Key words: homocysteine; elastin network; glass transition; thermal analysis; molecular mobility

INTRODUCTION

High plasma levels of homocysteine, a physiological sulfur-containing aminoacid, have been identified as an independent risk factor for atherosclerosis in many epidemiological studies.[1,2] Arterial lesions associated with hyperhomocysteinemia are characterized by intense extracellular matrix remodeling. One of the main features of this arterial remodeling is the degradation of the arterial elastin network. From histological and macroscopic point of view, this proteolytic process has been clearly characterized for arterial lesions occurring in homocystinuria,[3] the most severe form of hyperhomocysteinemia in humans, as well as in dietary-induced mild hyperhomocysteinemia in animals.[4,5] The degradation consists in an enlargement of physiological fenestrae in elastic laminae as a result of a protease dependant degradation of elastin network.[6] Raised MMP activity, calcification,[7] and impaired endothelial function are also associated with a high level of plasma homocysteine, which itself increases with age.[8]

The aim of this study was to characterize the influence of homocysteine on the physical structure and the molecular mobility of the arterial elastin network. To this end, we cultured arteries with concentrations of homocysteine matching physiological and pathological levels encountered in humans. The physical structure of the elastin network in cultured arteries was investigated by Differential scanning calorimetry (DSC) to analyze thermal transitions such as glass transition and denaturation. To explore the molecular dynamics of the elastin network in the nanometer range, we used thermally stimulated currents (TSC), a dielectric technique running at low frequency and measuring the dipolar reorientations in proteins subjected to a static electrical field.

Correspondence to: V. Samouillan; e-mail: vsamou@cict.fr

EXPERIMENTAL SECTION

Materials

Abdominal aortas were collected from young adult common pigs at a local slaughterhouse ($n = 6$)

and transferred to the laboratory at 4°C in flasks with phosphate buffered saline (PBS) containing antibiotic-antimycotic (10X-AB-AM : 1000 U/mL penicillin G, 1000 μg/mL streptomycin, 2.5 μg/mL amphotericin). Arteries were prepared under sterile conditions by gently removing the excess fat and interstitial tissue while avoiding stretching the artery or damaging the endothelium. Arterial explants (5-mm-long segments) were randomly put into culture dishes containing 10 mL serum free NCTC-135 medium[9] supplemented with 0.2% bovine serum albumin, 2X-AB-AM and homocysteine. Homocysteine was used both at 10 μ*M* corresponding to physiological homocysteinemia (Hcy10)[10,11] and at 100 μ*M* corresponding to severe hyperhomocysteinemia (Hcy100). The 12 arterial explants were then cultured at 37°C in a humidified incubator at 5% CO_2 for 72 h. At the end of culture, arterial explants were frozen and lyophilized. The lyophilized samples were then stored at 4°C, 50% relative humidity (RH) before physical analysis.

METHODS

Differential scanning calorimetry

The phase transition thermograms were recorded with a Perkin–Elmer DSC7 differential scanning calorimeter. The temperature and energy scales were calibrated using the manufacturer's instructions with Indium and Tin as standards. Freeze-dried arterial explants (5–10 mg in weight) were sealed in aluminum pans. Empty pans were used as references. Investigations were performed between 30 and 250°C with 20°C/min heating rates. Determination of transition parameters was performed with Origin software.

TSC—Global spectra

This technique was first used to characterize metallic divalent impurities in ionic crystals, and the was later applied to polymers because it allows dielectric relaxation processes to be scanned at a lower frequency than conventional dielectric spectroscopy.[12] The relaxations observed by TSC are largely due to the reorientation of polar groups or segments of the macromolecules.

TSC measurements were carried out with a dielectric apparatus developed in our laboratory and previously described.[13] Freeze-dried arterial explants (20–40 mg in weight) were compressed (2×10^3 kg/cm^2 during 2 min) resulting in disks 1 mm thick, 8 mm diameter. These samples were placed between two stainless steel plate electrodes. Before experiments, the sample cell was flushed and filled with dry He, to ensure good thermal exchange. To record complex spectra, the sample was polarized with a static electric field (E_p) at a given polarization temperature (T_p) for a time (t_p) long enough for the polarization to reach equilibrium. Then the sample was quenched by a cooling process to $T_0 \ll T_p$, allowing the orientation polarization [P(T_p)] to be frozen-in. Finally, the electric field was cut off and the sample was short-circuited for a time t_{cc} long enough to remove fast relaxing surface charges and to stabilize the sample temperature. The capacitor was then connected to a very sensitive electrometer (Keithley 642, 10^{-16} A accuracy). The depolarization current $I(T)$ induced by the linear increase in temperature ($T = qt + T_0$) was subsequently recorded against temperature, giving the relaxation spectrum of the sample. The peaks, which are associated with dipolar relaxations, must meet different criteria: their intensity must be proportional to the applied field, and the temperature maximum must be below T_p and stable at with different T_p values. In the present study, the polarization conditions resulting in reproducible dipolar relaxations were as follows: t_p = 2 min, E_p = 400 V mm^{-1}, t_{cc} = 2 min, and q = 7°C/min.

TSC—Fractional polarizations (FP)

In proteins, the TSC peaks corresponding to dipolar relaxations are in general too broad to be associated with only one single relaxation process, that is, with only one relaxation time. These broad peaks correspond to a distribution of relaxation times connected with the same dipolar mechanism. The FP procedure can be used to decompose a complex TSC peak in elementary processes contributing to a complex dielectric relaxation. In this procedure, each isolated spectrum is well approximated by a single relaxation time, accommodating Bucci–Fieschi's analysis.[14] In the FP procedure, the electrical field E_p is applied at T_p for 2 min, allowing the orientation of dipoles with relaxation time $\tau(T_p)$ lower than 2 min. The temperature is then lowered by ΔT to T_d (ΔT = 5°C) under field. At T_d, the field is turned off and the sample is then held for 2 min so that dipoles with relaxation time $\tau(T_d)$ lower than 2 min relax. The sample is then quenched to $T_0 \ll T_d$ so that only dipoles whose relaxation time $\tau(T)$ is such that $\tau(T_p) < 2$ min and $\tau(T_d) > 2$ min remain oriented at T_0. The depolarization current is recorded in a fashion similar to that mentioned earlier for the complex spectrum. The response of this FP experiment is the result of the reorientation of a narrow distribution of relaxation times excited over a ΔT = 5°C temperature window around T_p. By increasing the value of T_p by steps of 2.5°C along the temperature axis, the whole TSC spectrum is resolved into a series of fractional depolarization peaks, allowing us to reach experimentally the distribution of the global dipolar relaxation.

In Bucci–Fieschi's framework based on the conventional Debye treatment with a single relaxation time τ the reduction in polarization $P(t)$ after removal of the static field is given by:

$$P(t) = P_0 \exp[-t/\tau] \quad (1)$$

where P_0 is the saturation polarization. The corresponding depolarization current density $J(t)$ at time t is given by:

$$J(t) = -\mathrm{d}P(t)/\mathrm{d}t = P(t)/\tau \quad (2)$$

As the reduction in the frozen-in polarization is thermally stimulated, time and temperature are related by a

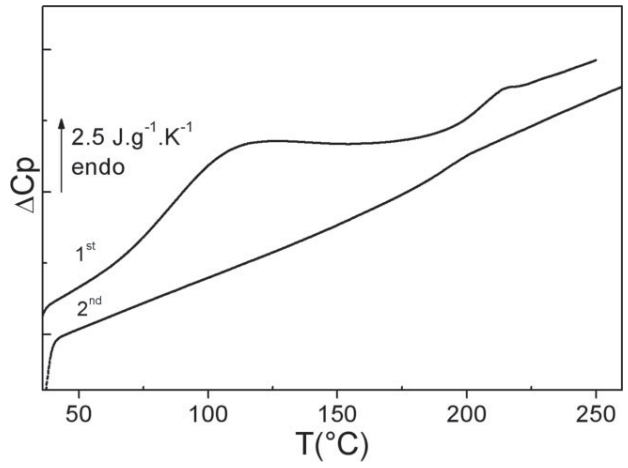

Figure 1. DSC thermogram of Hcy10 arterial explants (first and second scan).

linear relationship, $T = T_0 + q_t$, where q is the heating rate. The relaxation time τ is thus temperature dependent and can be written as:

$$\tau(T) = P(T)/J(T) \qquad \text{with} \quad P(T) = q^{-1}\int_{T}^{T} J(T')\mathrm{d}T' \qquad (3)$$

Therefore the temperature dependence of the relaxation time for an elementary peak can be deduced from the ratio between $I(T)$ and the remaining area under the peak from T to T_f, the temperature at which the depolarization current returns to zero.

Statistical analysis

The data are presented as means ± SD. Statistical analyses were performed using Student's t test.

RESULTS AND DISCUSSION

Thermal transitions

Figure 1 presents the DSC thermograms of an Hcy10 arterial explant. On the first scan, a broad endothermic peak is observed at 111°C; by analogy with previous studies on different proteins and connective tissues in the lyophilized state, this peak, which vanishes on the second scan, is attributed to the evaporation and vaporization of bound water adsorbed by the sample stored at 50–80% relative humidity.[15–17] Therefore, this thermal transition can be considered as an extrinsic transition and is generally evaluated by its temperature maximum (T_{max}) and its enthalpy, that is, the area under the curve (ΔH_{max}). As all the samples were stored in the same conditions (4°C, 50% RH), these two parameters can be used and compared to characterize the artery water uptake in these peculiar conditions.

A second thermal event, noted as a jump in the specific heat, appears between 190 and 220°C on the first and second scans: this reversible transition is associated with the glass transition of elastin in the freeze-dried state,[15,18] namely the transition from a vitreous to a rubbery state; by analogy with synthetic polymers, this intrinsic transition is characterized by its temperature (T_g), corresponding to the middle point of the specific heat jump of the step. The value of T_g is an important parameter of the chain dynamics of elastin, and gives specific information on the stiffness of the protein in the artery.

To evaluate the influence of a pathological concentration of homocysteine on cultured arteries, the thermograms corresponding to the first scan of Hcy10 and Hcy100 arterial explants ($n = 6$ for each concentration of homocysteine) were performed and superimposed on Figure 2. All the thermograms present both the broad transition associated with bound water departure and the glass transition of elastin, with different degrees of resolution. To facilitate comparison, the mean values and standard errors of the three parameters (T_{max}, ΔH_{max}, and T_g) of the two

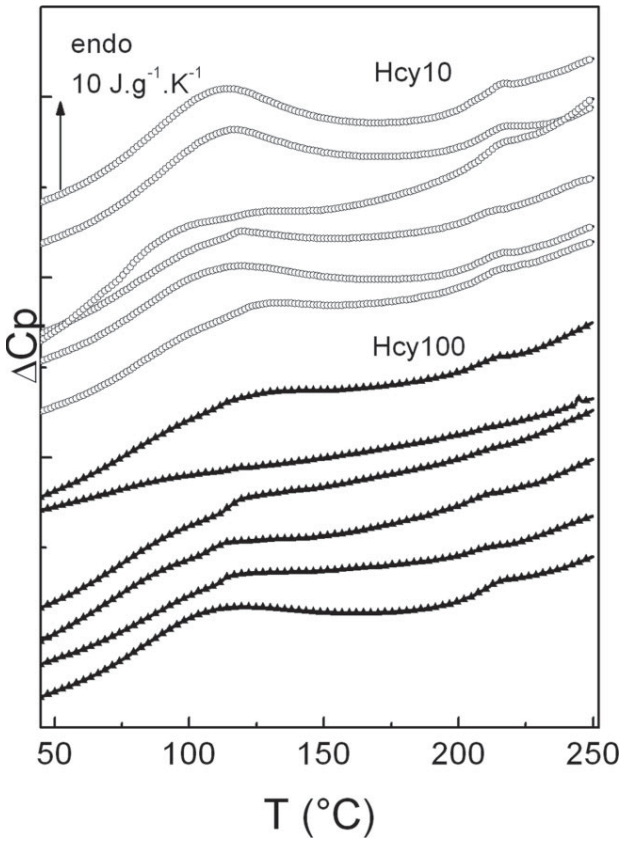

Figure 2. DSC thermograms of Hcy10 and Hcy100 arterial explants (first scan).

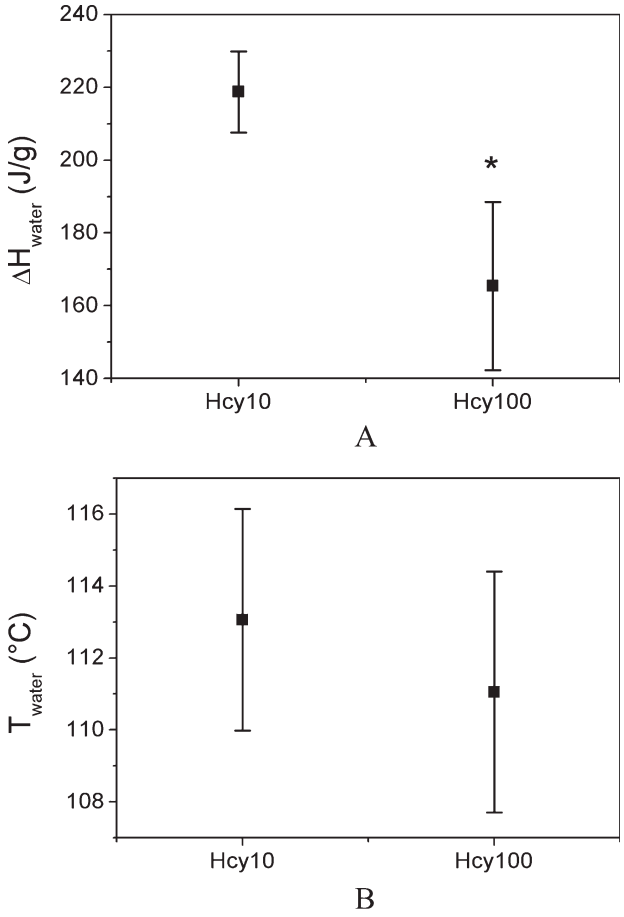

Figure 3. (A) Enthalpy of bound water departure from DSC thermograms (mean ± SD, n=6; *p = 0.05). (B) Temperature maximum of bound water departure from DSC thermograms (mean ± SD, n = 6).

transitions were extracted from the thermograms and are presented in Figures 3(A,B) and 4(A).

The most significant difference ($p < 0.05$) between the two groups of samples concerns the enthalpy associated with bound water loss. Bound water falls from 219 J g^{-1} for arterial explants cultured with 10 μ*M* homocysteine to 165 J g^{-1} for arterial explants cultured with 100 μ*M* homocysteine. This first difference suggests that Hcy10 arterial explants are more hydrated than the Hcy100 arterial explants; thermogravimetric measurements (not shown here) confirmed this assertion: levels of hydration were found to be (20 ± 1%) in Hcy10 arterial explants and (16 ± 1.5%) in Hcy100 arterial explants, respectively.

In contrast to enthalpy values, the temperature maxima of the extrinsic transition are not significantly different for the two kinds of samples, which indicate that water is fixed on similar sites in both cases. Previous works on hydrated and dehydrated elastin[15] assign this water to nonfreezable water, H-bonded to amine and carbonyl groups of the polypeptidic chain of elastin. The slight but significant fall of hydration in Hcy100 arterial explants can be associated to a rearrangement of the hydrogen bond network with Hcy. It certainly reflects a modification in the ratio of secondary structures in elastin such as random coil, β turns and α helices, known as labile conformations in elastin and associated polypeptides.[19]

There is a slight difference ($p = 0.05$) in the glass transition of elastin for the two sets of samples; T_g varies from 206.4 to 205.6°C for arterial explants cultured with 10 and 100 μ*M* homocysteine, respectively. By analogy with synthetic polymers,[20] this slight but significant decrease in T_g reveals a softening of elastin in arteries cultured in physiopathological conditions, namely a fall of the mechanical properties.

Another important factor is brought to light with the detailed analysis of the thermal transitions of freeze-dried arteries in Figure 2: we observe that some thermograms are characterized by an additional jump in the specific heat at around 115°C; this transition, which appears with more accuracy on the T-derived curves, was identified on each thermogram. Figure 4(B) gives a detailed account of this

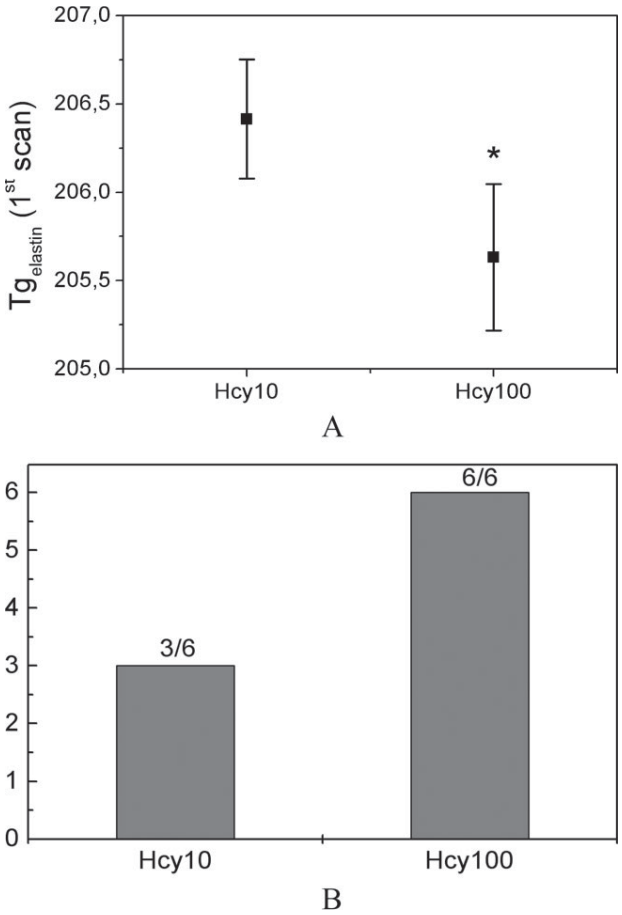

Figure 4. (A) Glass transition temperature of elastin from DSC thermograms (mean ± SD, n=6; *p = 0.05). (B) Occurrence of an additional glass transition at 115°C (from DSC thermograms).

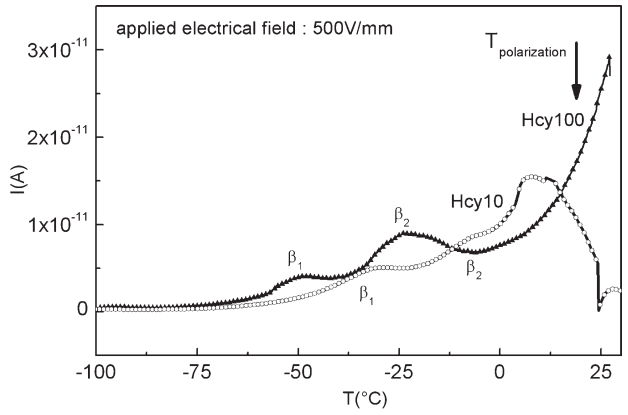

Figure 5. Global TSC spectra of Hcy10 and Hcy100 arterial explants in the low temperature range.

additional transition for each set of samples. This transition reappears twice for arterial explants cultured with 100 μ*M* homocysteine. Moreover, the analysis of the T-derivated curves highlights a more intense peak associated with this thermal event for the Hcy100 arterial explants when compared with the Hcy10 arterial explants ones (0.07 and 0.04 arbitrary units, respectively). The thermal characteristic of this transition suggests a pseudo-second-order transition, namely a glass transition: the occurrence of a new glass transition in arterial explants is thus attributed to a new amorphous component, whose origin needs to be determined. By comparison with extensive data on the jump in the specific heat in synthetic polymers,[21] the value of the jump of ΔC_p (0.2–0.5 J K^{-1} g^{-1}) indicates that a large quantity of this amorphous component is present in the arteries. Neither proteins present in small quantities in arteries, nor possible elastin fragments resulting from elastin hydrolysis in cultured arterial explants can explain this transition. Previous studies by DSC on kappa-elastin and enzymatically digested elastins showed that the glass transition of elastin was strongly dependent on the molecular architecture of this protein.[22] As a matter of fact, the temperature of this glass transition significantly decreases with a high degree of chemical or enzymatic digestion. Therefore, we suggest this thermal event, which is emphasized with pathological concentrations of homocysteine, is associated with a new phase of elastin, corresponding to a degraded network. It is noteworthy that if we apply this hypothesis, two phases of elastin corresponding to intact network and impaired network coexist in arterial explants cultured with 100 μ*M* homocysteine.

Dielectric relaxations

Dielectric analysis of cultured arterial explants is an additional tool to determine with greater accuracy the chain dynamics of the major proteins in these samples. Figure 5 presents the global TSC spectra of Hcy10 and Hcy100 arterial explants obtained after a polarization temperature of 20°C with a static electrical field of 500 V mm^{-1}, and illustrates the dipolar mobility of the major proteins of arteries in the low temperature range. We present a representative spectrum for each set of samples to simplify the figure. The TSC spectrum of Hcy10 arterial explants is characterized by two dipolar relaxations that appear as shoulders (labeled β_1 and β_2) at -31 ± 2°C and -8 ± 3°C, respectively. By analogy with TSC studies on a large series of biological and synthetic polymers,[23–27] the intensity and temperature position of the β_1 and β_2 modes indicate a link with localized movements of the polypeptidic chains. Previous dielectric studies on various connective tissues in the freeze-dried state have indeed linked these two relaxations to the reorientation of polar groups of some nanometers along elastin and collagen backbone.[27]

The TSC spectrum of Hcy100 arterial explants also presents these two relaxation modes, which appear as peaks and not shoulders at -49 ± 4°C and -23 ± 3°C, respectively. The intensity of the two modes is relatively similar in Hcy10 and Hcy100 arterial explants, but a major difference is observed in the temperature position of the relaxations: the TSC spectrum of Hcy100 arterial explants is largely shifted toward low temperature, which indicates plastification. The shift in relaxations toward low temperature is generally interpreted as an increase in molecular mobility of the dipolar groups involved. In TSC experiments, dipolar reorientations are thermally activated: thus, the greater is the energy requirement for the movement, the greater the temperature. In accordance with the thermal results, the difference in global dielectric behavior

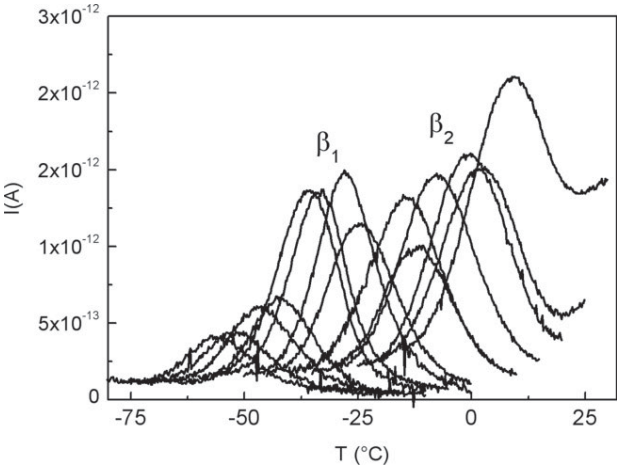

Figure 6. Experimental decomposition of the low temperature spectrum of Hcy10 arterial explants (FP procedure).

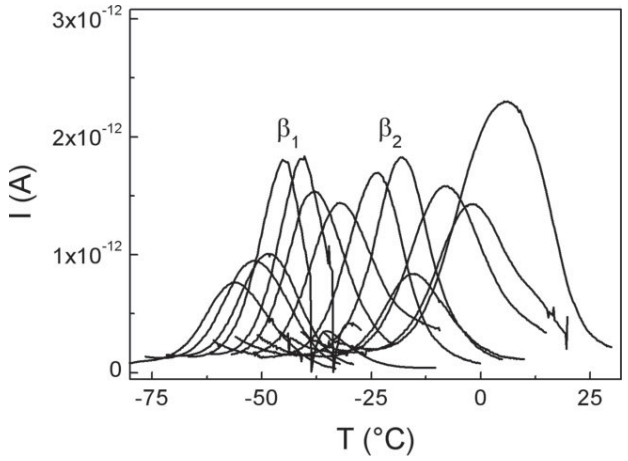

Figure 7. Experimental decomposition of the low temperature spectrum of Hcy100 arterial explants (FP procedure).

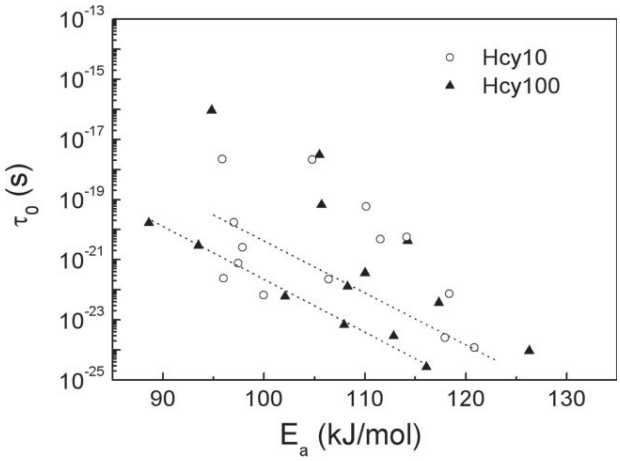

Figure 8. Compensation diagram of Hcy10 and Hcy100 arterial explants in the low temperature range.

between the two groups of arterial explants reinforces the degrading effect of 100 μ*M* homocysteine on the arterial elastin network.

To define more clearly the influence of pathological concentrations of homocysteine on the local chain dynamics of proteins, the technique of fractional polarizations was performed on each set of samples in the low temperature range, according to the protocol described in the experimental section.

Figure 6 shows the set of elementary spectra obtained for Hcy10 arterial explants when the polarization window is displaced from −65 to 0°C. The sum of these peaks reproduces the global TSC spectrum: the FP procedure allows us to perform an experimental decomposition of the global relaxation in elementary relaxations, corresponding to single relaxation times as described in Eq. (3). The same FP protocol was applied to Hcy100 arterial explants; the experimental decomposition is presented in Figure 7. In this case too, the sum of the elementary peaks fits the global spectrum, and the β_1 and β_2 modes can be detected.

Bucci–Fieschi's framework based on the conventional Debye treatment was used to determine the temperature dependence of each relaxation time associated with an elementary peak following Eq. (3), and thus to access the experimental distribution of relaxation times in the low temperature range for the two kinds of arteries. When the variation of $\tau(T)$ was plotted versus temperature, we noted that all the extracted relaxation times are well fitted by an Arrhenius law:

$$\tau_i(T) = \tau_{0i} \exp(E_{a_i}/RT) \tag{4}$$

where τ_i is the isolated relaxation time from the ith peak, T the temperature, τ_{0i} an exponential factor, E_{ai} the activation energy, and R the ideal gas constant.

This result is in good agreement with previous studies on the local chain dynamics of polymers, which generally present an Arrhenius dependence for the relaxation time associated with sub-T_g movements. This temperature dependence can be interpreted in terms of Eyring's activated state rate theory where $\tau(T)$ follows the law:

$$\tau_i(T) = \frac{h}{KT} \exp\left(\frac{-\Delta S_i}{R}\right) \exp(\Delta H_i/RT) \tag{5}$$

where ΔS_i and ΔH_i are the activation entropy and the activation enthalpy of an elementary dipolar reorientation, respectively, k Bolzmann's constant and h Plank's constant.

The local chain dynamics of the Hcy10 and Hcy100 arterial explants are thus well represented by Figure 8, where we plot the variation of pre-exponential factor (τ_0 vs. the activation energy E_a for each elementary peak in a semilogarithmic scale. In both Hcy10 and Hcy100 arterial explants, a linear relationship is observed for the parameters associated

TABLE I
Parameters of the Linear Fit $\log\tau_0 = A + BE_a$ (from Figure 8)

	A	ΔA	B	ΔB	R	N	SD	p
Hcy10	−4.67	1.08	-1.597×10^{-4}	9.37×10^{-6}	−0.99828	4	0.10136	0.00226
Hcy100	−4.13	0.36	-1.763×10^{-4}	3.56×10^{-6}	−0.99939	5	0.07835	<0.0001

TABLE II
Compensation Parameters of the β1 Mode

	T_c (°C)	ΔT_c (°C)	τ_c (s)	Energy Range (kJ mol^{-1})
Hcy10	54	19	2×10^{-5}	From 97 to 121
Hcy100	23	6	7×10^{-5}	From 88.5 to 116

with the β1 mode and can be expressed by the following equation:

$$\log(\tau_{0i}) = a + bE_{ai} \tag{6}$$

where a is the origin ordinate and b the slope of the straight line, respectively. These parameters with their associated errors are reported in Table I for the two sets of points.

This relationship can be also written as follows:

$$\tau_{0_i} = \tau_c \exp\left(\frac{E_{ai}}{RT_c}\right) \tag{7}$$

where $\tau_c = 10^a$ and $T_c = -1/(bR\ln 10)$.

At temperature T_c, all the related relaxation times would have the same value τ_c, which is considered in the literature as a compensation phenomenon.[27–29] We present in Table II the values of T_c and τ_c for Hcy10 and Hcy100 arterial explants, giving a good indication of the size of the implied movements. By analogy with previous studies on wide range of polymers,[28] the values of τ_c, in the order of 10^{-5} s in both cases, can be associated with local movements of some nanometers along the polypeptide chain. Values for T_c are significantly different between the Hcy10 and Hcy100 arterial explants; in fact decrease in T_c for 100 μ*M* homocysteine reflects the behavior of the global β1 mode, which was shifted toward low temperature; the plastification of the local chain dynamics at this pathological concentration of homocysteine is therefore confirmed. Another interesting point is related to the energy distribution range of the elementary processes involved in the β1 mode (Table II). This energy range is shifted toward low values in Hcy100 arterial explants: in agreement with the William–Hoffman–Passaglia theory,[30] the reorienting dipolar sequences are smaller in Hcy100 arterial explants than in Hcy10 arterial explants. This information is in good agreement with the previous hypothesis from DSC results regarding a possible fragmentation of the elastin network. In fact, the formation of hanging chains subsequent to a degradation process could explain such a shift in energy distribution in the β1 mode, and could also be responsible for plastification. It is important to note that a similar shift in energy distribution was observed on the main mode of the elastin network from bovine arteries degraded by elastases.[18]

A final important point of comparison between the local chain dynamics of the two cultured arterial explants concerns the value of the pre-exponential factor, τ_0, which is related to the activation entropy by the following formulae [combination of Eqs. (4) and (5)][31]:

$$\tau_{0_i} = \frac{h}{KT}\exp\left(\frac{-\Delta S_i}{R}\right) \tag{8}$$

Figure 8 shows that the τ_0 values for the β1 mode of Hcy100 arterial explants are lower than the τ_0 values for Hcy10 arterial explants; when considering Eq. (8), this decrease in τ_0 is necessarily linked in to an increase in the activation entropy. Activation entropy is related to the number of conformations accessible for the dipolar group and its environment in the activated state leading to reorientation. An increase in this number is thus an indication of local disorder around the dipolar sequence when it reorientates.

CONCLUSION

In this study, we show that high levels of homocysteine significantly impair the physical properties of the elastin network in cultured arteries. Suggesting degradation of the elastin network, these results give new insights into the well-known degradation of the elastic structures in the arterial wall associated with hyperhomocysteinemia.[4] Elevated plasma homocysteine has been associated with cardiovascular disease, although a causal relationship is still unclear at this time.[32] Our results seem to corroborate recent studies showing that Hcy activates matrix metalloproteinase (MMP), leading to elastin network disruption.[33] Nevertheless, other studies—suggesting that elevated plasma methionine or its metabolites disrupt normal microfibril configuration, leading to the assembly of aberrant elastic fibers[34]—need not be neglected, and further investigations will be necessary to clarify the structural modifications of elastin network in presence of homocysteine. These molecular alterations could account, at least in part, for the impairment of arterial rheology in hyperhomocysteinemic patients.[35,36]

References

1. McCully KS. Homocysteine, folate, vitamine B6 and cardiovascular disease. Atheroscler Rev 1983;11:157–246.
2. Eikelboom JW, Lonn E, Genest J, Hankey G, Yusuf S. Homocyst(e)ine and cardiovascular disease: A critical review of the epidemiologic evidence. Ann Intern Med 1999;131:363–375.
3. Gibson JB, Carson NA, Neill DW. Pathological findings in homocystinuria. J Clin Pathol 1964;17:427–437.

4. Rolland PH, Friggi A, Barlatier A, Piquet P, Latrille V, Faye MM, Guillou J, Charpiot P, Bodard H, Ghiringhelli O. Hyperhomocysteinemia-induced vascular damage in the minipig: Captopril-hydrochlorothiazide combination prevents elastic alterations. Circulation 1995;91:1161–1174.
5. Augier T, Charpiot P, Chareyre C, Remusat M, Rolland PH, Garcon D. Medial elastic structure alterations in atherosclerotic arteries in minipgs: Plaque proximity and arterial site specificity. Matrix Biol 1997;15:455–467.
6. Charpiot P, Bescond A, Augier T, Chareyre C, Fraterno M, Rolland PH, Garcon D. Hyperhomocysteinemia induces elastolysis in minipgs arteries: Structural consquences, arterial site specificity and effect of captopril-hydrochlorothiazide. Matrix Biol 1998;17:559–574.
7. Van Campenhout A, Moran CS, Parr A, Clancy P, Rush C, Jakubowski H, Golledge J. Role of homocysteine in aortic calcification and osteogenic cell differentiation. Atherosclerosis 2009;202:557–566.
8. Greenwald SE, Martin JE, Sheaff MT. Ageing of the conduit arteries. The pathology of ageing: Concepts and mechanisms. J Pathol 2007;211:157–172.
9. Barrett LA, Mergner WJ, Trump BF. Long-term culture of human aortas: Development of atherosclerotic-like plaques in serum-supplemented medium. In Vitro 1979;15:957–966.
10. Scazzone C, Acuto S, Guglielmini E, Campisi G, Bono A. Methionine synthase reductase (MTRR) A66G polymorphism is not related to plasma homocysteine concentration and the risk for vascular disease. Exp Mol Pathol 2009;86:131–133.
11. Huang L, Song XM, Zhu WL, Li Y. Plasma homocysteine and gene polymorphisms associated with the risk of hyperlipidemia in northern Chinese subjects. Biomed Environ Sci 2008;21:514–520.
12. Van Turnhout J. Thermally Stimulated Discharge of Polymer Electrets. Amsterdam: Elsevier Scientific Publishing Company; 1975.
13. Teyssedre G, Mezghani S, Bernes A, Lacabanne C. Thermally stimulated currents of polymers. In: Runt JP, Fitzgerald JJ, editors. Dielectric Spectroscopy of Polymeric Materials. Fundamental and Applications. Washington DC: American Chemical Society; 1997. p 227–255.
14. Bucci C, Fieshi R. Ionic thermocurrents in dielectrics. Phys Rev Let 1964;12:16–19.
15. Samouillan V, Andre C, Dandurand J, Lacabanne C. Effect of water on the molecular mobility of elastin. Biomacromolecules 2004;5:958–964.
16. Puett D, Ciferri A, Rajagh LV. DTA and heats of hydration of some polypeptides. Biopolymers 1965;3:439–459.
17. Samouillan V, Dandurand-Lods J, Lamure A, Maurel E, Lacabanne C, Gerosa G, Venturini A, Casarotto D, Gherardini L, Spina M. Thermal analysis characterization of aortic tissues for cardiac valves bioprostheses. J Biomed Mater Res 1999; 46:531–538.
18. Samouillan V, Lamure A, Maurel E, Lacabanne C, Hornebeck W. Alterations in the chain dynamics of insoluble elastin upon proteolysis by serine elastases. Biopolymers 2001; 58:175–185.
19. Tamburro AM, Pepe A, Bochicchio B. Localizing α-helices in human tropoelastin: Assembly of the "Elastin Puzzle". Biochemistry 2006;45:9518–9530.
20. Jaffe M, Menczel JD, Bessey W. E. Thermal Characterization of Polymeric Materials. New York: Academic Press; 1997.
21. Wunderlich B. Thermal Analysis. Boston: Academic Press; 1990.
22. Samouillan V, Dandurand J, Lacabanne C, Hornebeck W. Molecular mobility of elastin: Effect of molecular architecture. Biomacromolecules 2002;3:531–537.
23. Pathmanathan K, Cavaillé JY, Johari GP. The effects of increased crystallization on the electrical properties of nylon 12. J Polym Sci Part B: Polym Phys 1992;30:341–348.
24. Andrady AL, Mark JE. Dynamic mechanical properties relaxations in swollen elastin networks. Polym Bull 1991; 27:227–234.
25. Le Huy, HM Rault J. Remarks on the alpha and beta transitions in swollen polyamides. Polymer 1994;35:136–139.
26. Bone S, Pethig R. Dielectric studies of protein hydration and hydration-induced flexibility. J Mol Biol 1985;181:323–326.
27. Samouillan V, Lamure A, Maurel E, Dandurand J, Lacabanne, C Spina M. Dielectric characterization of collagen, elastin and aortic valves in the low temperature range. J Biomater Sci Polym Ed 2000;11:583–598.
28. Lavergne C, Lacabanne C. A review of thermo-stimulated current. IEEE Elec Insul Mag 1993;9:5–21.
29. Crine JP. Rate theory and PE relaxations. IEEE Trans Elec Ins 1987;EI22:169–174.
30. Hoffmann JD, Williams G, Passaglia EJ. Analysis of the a, b and g relaxations in polychlorotrifluoroethylene and polyethylene: Dielectric and mechanical properties. Polym Sci 1966;C14:173–235.
31. Eyring HJ. Viscosity, plasticity and diffusion as examples of absolute reaction rates. Chem Phys 1936;4:283–291.
32. Neves MF, Endemann D, Amiri F, Virdis A, Quian Pu Rozen R, Schiffrin EL. Small artery mechanics in hyperhomocysteinemic mice: Effects of angiotensin II. J Hypertens 2004; 22:959–966.
33. Rosenberger D, Moshal KS, Kartha GK, Tyagi N, Sen U, Lominadze D, Maldonado C, Roberts A, Tyagi SC. Arrhythmia and neuronal/endothelial myocyte uncoupling in hyperhomocysteinemia. Arch Physiol Biochem 2006;112:219–227.
34. Hill CH, Mecham R, Starcher B. Fibrillin-2 defects impair elastic fiber assembly in a homocysteinemic chick model. J Nutr 2002;132:2143–2150.
35. Nestel PJ, Chronopoulos A, Cehun M. Arterial stiffness is rapidly induced by raising the plasma homocysteine concentration with methionine. Atherosclerosis 2003;171:83–86.
36. Rodrigo R, Passalacqua W, Araya J, Orellana M, Rivera G. Homocysteine and essential hypertension. J Clin Pharmacol 2003;43:1299–1306.